Available online at www.sciencedirect.com

ScienceDirect

IFAC Papers Online CONFERENCE PAPER ARCHIVE

IFAC PapersOnLine 53-2 (2020) 2796–2801

Robustness of event-based discrete PI controllers. A sampled describing function approach ⋆

Oscar Miguel-Escrig * **Julio-Ariel Romero-Pérez** **

*Department of Engineering and Design. Universitat Jaume I. Campus del Riu Sec Avda. Vicent Sos Baynat s/n 12071. Castellón. Spain. (e-mail: * omiguel@uji.es, ** romeroj@uji.es).*

Abstract:
In this paper we present a study about the robustness of event-based discrete PI controllers. Our approach is based on Sampled Describing Function technique, which has been used to characterize the non-linear effect of the Symmetric Send on Delta (SSOD) sampling strategy on the control loop. Through several examples this technique is proven to produce accurate results in predicting limit cycle oscillations and to provide guidelines to avoid them, either by detuning the controller or increasing the sampling period.

Keywords: Event-based Control, Sampled Describing Function, SSOD, robustness

1. INTRODUCTION

On distributed control systems, event based controllers are a promising alternative to classical time driven approach because the former allows to reduce the data flow through digital networks, reducing the data drop out in the form of packet losses and decreasing the delays introduced by the communication network. This is due to the characteristics of event based control systems (EBC) of sending new data only when significant changes are detected on the state of the system, instead of the periodical sampling required by the classical time-driven control loops.

Specially important in the EBC is the event generation technique, which is in charge of generating the events for the execution of the controller's algorithm. Among these sampling strategies the ones based on the signal quantification have become more important because of their ease of implementation. One of the most important is the send-on-delta (SOD) sampling, which sends data whenever the signal changes more than a value δ from the last sample. This sampling technique has been used in several works proving its effectiveness in terms of control performance and communication reduction (Dormido et al. [2008], Ploennigs et al. [2010]). A variation of SOD was presented in (Beschi et al. [2012]) known as symmetric-send-on-delta (SSOD), which fixes the thresholds δ and introduces a hysteresis of the same value δ.

One of the main points in the analysis and design of event-based control systems is the existence and avoidance of limit cycle oscillations in the closed loop response. To perform this analysis, the Describing Function (DF) technique has been applied in previous works by the authors (Romero et al. [2014], Romero and Sanchis [2016]), obtaining tuning methods for PI controllers within a structure with a SSOD sampler. The use of the DF allows to extend some concepts of the classical control theory, such as the gain and phase margins, to the analysis and design of EBC systems.

Until now, in all the published studies about the SSOD based control systems a continuous approach is adopted towards the controller implementation (Beschi et al. [2014], Romero et al. [2014]), i.e. the controller is considered to be continuous and therefore all the results have been obtained under this assumption. In networked control systems, however, the controller is implemented in micro-processor based devices considering a discrete approximation where the execution period plays an important role.

In this paper we address the robustness of SSOD based control systems when using discrete PI controllers. The approach consists in assuming the PI to be implemented in any standard control device (PLC, microcontroller,...), as is almost always the case in actual applications, and no longer considering it as a continuous controller. The results shed light on the importance of the sampling period on the robustness against limit cycle oscillations and prove the suitability of the Sampled Describing Function technique to analyze this kind of systems.

2. PROBLEM STATEMENT

Consider the networked control system presented in Figure 1, where $C(s)$ and $G(s)$ are the controller and the process transfer functions respectively, y_r is the reference signal to be tracked, y is the controlled output, and p is the disturbance input. It is supposed that the controller is located near the actuator and the sensor sends measurements of process output y (or more precisely of the tracking error e) to the controller through a communication network using the SSOD strategy. The ZOH block keeps in $\bar{e}$ the last sent value of process output e^* until a new value is transmitted

⋆ This work has been supported by the projects UJI-B2018-39 and ACIF/2018/244.

10.1016/j.ifacol.2020.12.943

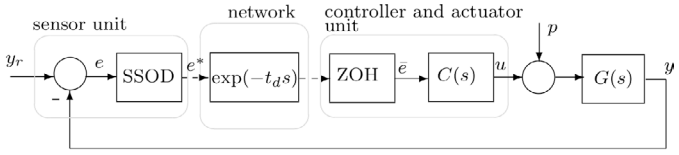

Fig. 1. Networked control system with SSOD sampling strategy.

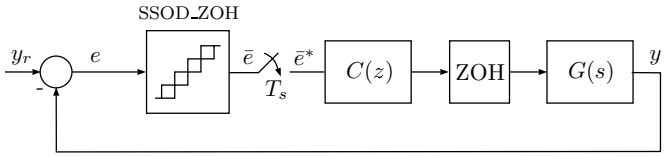

Fig. 2. Sampled system configuration with SSOD non-linearity.

by the SSOD block. Communication delays through the network are represented by the term $\exp(-t_d s)$.

The control problem associated to this schema was first proposed in (Beschi et al. [2012]) and it has been treated in different ways in the literature. In (Beschi et al. [2014]) a tuning method for this kind of structure based on AMIGO (Hägglund and Åström [2002]) and SIMC (Skogestad [2003]) tuning rules was presented. In (Romero et al. [2014], Romero and Sanchis [2016]) the authors use the DF technique to characterize the robustness of the SSOD non-linearity and propose their own tuning method, but other analysis tools can be used to better characterize the system behavior (Miguel-Escrig et al. [2019]).

All the previous works consider a continuous controller $C(s)$, but in practice the PI is implemented in microprocessor based devices such a PLC or other electronic cards. This fact modifies the system in Figure 1, because the signal $\bar{e}$ is now periodically sampled by the controller to recalculate the control action, which keeps constant during the sampling time.

With the considerations described above, the system in Figure 1 admits the Hammerstein-Wiener representation presented in Figure 2, being the block SSOD_ZOH the combination of the SSOD and ZOH blocks, the network delay has been included in the process transfer function $G(s)$, and the implementation of the dicrete PI being modeled by

$$C(z) = K_p + K_p \frac{T_s}{T_i} \frac{z}{z-1}. \tag{1}$$

This configuration represents more accurately the actual problem behind the implementation of networked control systems. A possible drawback of this kind of systems is the existence of limit cycles induced by the SSOD sampling. In Figure 3 a limit cycle oscillation is shown, and it can be seen that, the error signal e is not only quantified by the SSOD non-linearity, resulting in $\bar{e}$, but also sampled afterwards, obtaining the samples $\bar{e}^*$, which are used to compute and actualize the control action.

3. SAMPLED DESCRIBING FUNCTION

According to (Gelb and Van der Velde [1968]), for non linear systems that include sampling elements, as that

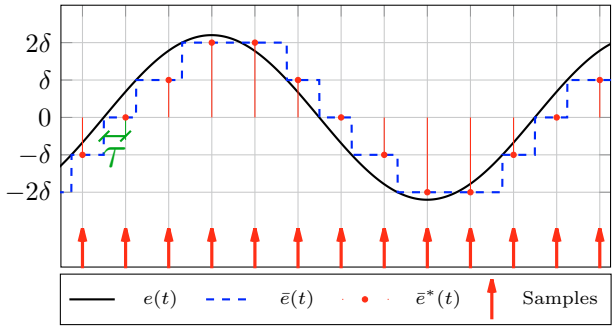

Fig. 3. Sine wave in black, quantified by the SSOD_ZOH block in dashed blue, and sampled according to a given sampling period in red (sampling time indicated with red arrows).

in Figure 2, two extensions of the Describing Function technique can be used to study the existence of limit cycles: the z-transform describing function and the sampled describing function. Due to its simplicity we have chosen the later approach for this work.

The condition to avoid limit cycle oscillations is defined by:

$$G_{ol}(j\omega) \neq -\frac{1}{\mathcal{N}}; \quad \forall\omega, \tag{2}$$

where $G_{ol}(j\omega)$ represents the open-loop transfer function including the controller, the process and the ZOH. $\mathcal{N}$ is the sampled describing function that characterizes the SSOD_ZOH block and the sampler.

$\mathcal{N}$ is calculated according to the expressions presented in Appendix A. From those expressions it can be concluded that the shape of $1/\mathcal{N}$ is affected by the number of levels m crossed by oscillations with amplitude A ($m = \lfloor A/\delta \rfloor$), the lag τ introduced by the sampling (see Figure 3) and the ratio between the oscillation period and the sampling period $r = T_o/T_s = \omega_s/\omega_o$. Specially important is the effect of the sampling period T_s, which proportionally scales $\mathcal{N}$.

Figure 4 shows the shape of $-1/\mathcal{N}$ for different values of r. As can be observed, the locus of $-1/\mathcal{N}$ is composed of several branches, one for each value of m. Higher values of m tend to approximate the corresponding branches to the point $(-T_s, 0)$. On the other hand, as m is reduced the branches expand towards the third quadrant. A very illustrative case is the one presented in the Figure 4d, where the branches for each m are well defined and reassembles the DF of the SSOD without periodical sampling that was presented by the authors in (Romero and Sanchis [2016]). This happens because for values of r high enough the effect of the sampling can be negligible. Nevertheless, it can be seen how decreasing r tends to widen the branches, making them unintelligible from one another.

Remark 1. According to (Gelb and Van der Velde [1968]), for non-integer values of r the oscillation may contain harmonic components with frequencies lower than the fundamental frequency, which cannot be discarded with the filtering hypothesis, making the DF technique not suitable for the analysis of the system. Therefore, this approach only predicts the oscillation corresponding to integer values of r.

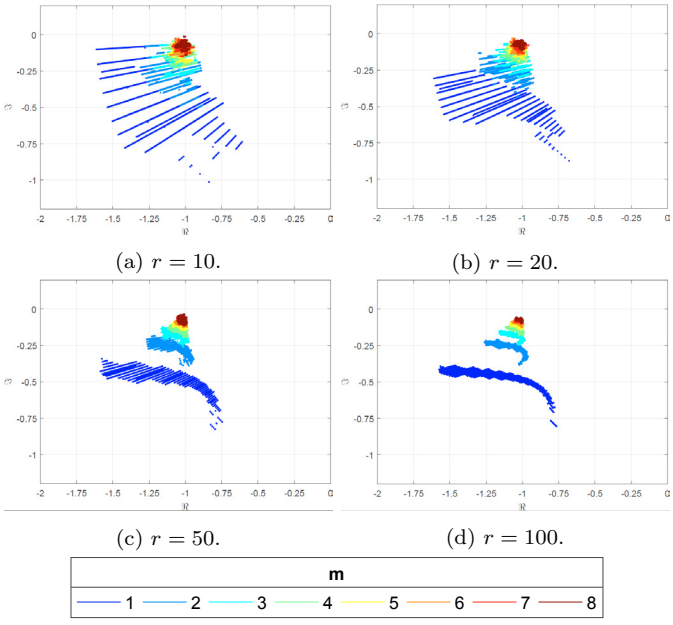

(a) $r = 10$. (b) $r = 20$. (c) $r = 50$. (d) $r = 100$.

Fig. 4. Sampled DF traces for different values of r, all of them considering $T_s = 1$.

Remark 2. In those cases where r is considered to be odd, the samples taken in each semi-period of the oscillation are different, affecting the symmetry of the oscillation, and therefore, the resemblance of the error signal $e(t)$ with a ideal sinusoid. Nevertheless, with a linear part with good filtering capabilities the DF still provides good results in predicting limit cycles.

4. STABILITY ANALYSIS

The condition (2) means that if there are not intersections between $G_{ol}(j\omega)$ and $-1/\mathcal{N}$ in a polar plot diagram, then cycle limit oscillations will not take place. With regard to the non-linear part, the fact that all the range of ω should be considered for the stability analysis implies that, for a given sampling period, different values for the ratio r must be considered since each frequency ω is susceptible of becoming the oscillation frequency.

Nevertheless, the range of ω, and thus, the range of r, can be easily calculated. Firstly, since the DF traces lie in the third quadrant, the minimum value of r which has to be considered is $r_{min} = \lceil \omega_s/\omega_{cp} \rceil$, where ω_{cp} is the phase crossover frequency. Secondly, as it has been seen in Figure 4, increasing r more than a certain value does not modify significantly the shape of the DF traces. In addition, the intersection between the traces of the DF and $G_{ol}(s)$, in the case where it happens, occurs in a given range of frequencies, therefore, the minimum possible oscillation frequency to consider, which will produce the maximum value for r, will be placed in the third quadrant, but not further than the extension of the DF traces.

With regard to the linear part of the system in Figure 2, the open loop transfer function $G_{ol}(s)$ that includes the discrete controller $C(z)$, the ZOH and the system $G(s)$ must be obtained. The transfer function of the ZOH is:

$$ZOH(s) = \frac{1 - e^{-sT_s}}{s}.$$

Furthermore, for the transfer function of the discrete controller, given by equation (1), its starred transfer function $C^*(s)$ is obtained by doing the transformation $z = e^{sT_s}$ on $C(z)$. Then:

$$G_{ol}(s) = \frac{1 - e^{-sT_s}}{s} C^*(s) G(s). \tag{3}$$

Due to the characteristics of $-1/\mathcal{N}$ described in the previous section, for PI controllers with reasonable tuning in terms of phase and gain margin, the shape of $G_{ol}(s)$ is generally such that the non intersection with the branches of $m = 1$ guarantees no intersections for $m > 1$. This fact was pointed out in (Romero and Sanchis [2016]) for the case of continuous PI and it holds for the system under study in this paper. Therefore, only the branches of $m = 1$ need be considered.

5. SIMULATION STUDY

To clarify the analysis of robustness to limit cycles of the system in Figure 2 using the concepts presented until now, let us introduce the following examples.

Example 1. Consider a process whose transfer function is:

$$G(s) = \frac{1}{(s+1)^3}.$$

A continuous PI controller is tuned according to the method proposed in (Romero and Sanchis [2016]), which takes into account the SSOD sampling strategy. The requirements are set to $\Phi_{m,SSOD} = 15°$ for the phase margin to the non-linearity and $\gamma_{cg} = 6$ dB for the gain margin, obtaining the following parameters: $K_p = 1.28$ and $T_i = 2.52$. It is worth remarking that implementing the continuous controller with these parameters assures the avoidance of limit cycle oscillations.

Now consider a discrete implementation of the PI controller using the previous parameters. To show the influence of this kind of implementation the sampling period has been chosen to be $T_s = 0.75$ seconds. The open loop transfer function obtained from equation (3) has a phase crossover frequency of $\omega_{cp} = 1.06$. Therefore, the possible frequency of limit cycles are lower than this value, which makes $T_{cp} = 5.9236$ and thus the initial value of $r_{min} = \lceil T_{cp}/T_s \rceil = \lceil 5.9236/0.75 \rceil = \lceil 7.8982 \rceil = 8$. The following values of r to consider will be greater because as we consider frequencies deeper on the third quadrant this ratio increases. As it has been commented before, as r increases, the variation between Sampled DF's traces is minor, so it is not necessary to sweep all the possible range of frequencies.

A quantification threshold $\delta = 0.1$ will be considered for the sampler in all the examples. In Figure 5 it can be seen the traces of $-1/\mathcal{N}$ for $r \in [8, 16]$ and $G_{ol}(s)$. As it can be appreciated it exists an intersection between the DF traces and $G_{ol}(s)$ and therefore a limit cycle oscillation can occur.

The system has been tested in simulation and effectively it presents a limit cycle oscillation as it can be seen in Figure 6. The controlled output of the system to step changes in reference and disturbance inputs can be seen in the upper figure and the respective control action is presented

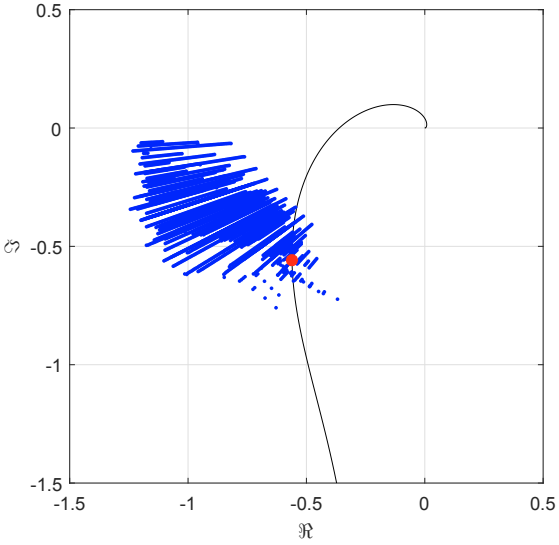

Fig. 5. Intersection between the traces of $-1/\mathcal{N}$ and $G_{ol}(s)$ with $T_s = 0.75$. Oscillation point showed in red.

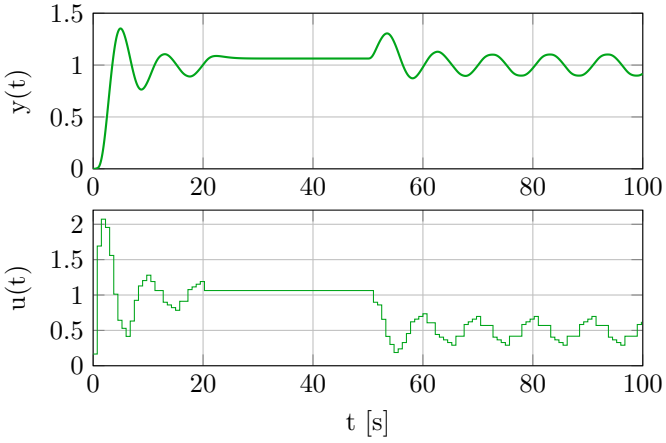

Fig. 6. Experiment considering step changes in the reference and disturbance inputs. Controlled output in the upper figure and control action in the lower figure.

in the lower image. Here, effectively, a limit cycle can be observed and its oscillation frequency $\omega_o = 0.5984$ [rad/s] correspond to the red dot in Figure 5.

As we have seen in the precedent example, the choice of the sampling period T_s and the tuning parameters is not trivial, even in those systems where this choice seems reasonable. The limit cycle oscillations presented are a direct consequence of this choice, because this controller implemented in a continuous form, i.e. without the sampling, does not make the system enter an oscillatory state.

In most applications, the sampling period is a system restriction, and thus it cannot be changed. For those kind of systems the solution to avoid limit cycle oscillations is to detune the controller, by reducing K_p until no intersection with the traces of the DF are observed. The key point here is that reducing K_p results in a radial shrink of $G_{ol}(s)$ without changing the frequencies at a given phase $\arg(kG_{ol}(j\omega)) = \arg(G_{ol}(j\omega))$, $k \in \Re^+$. This implies that the range of r does not change, and therefore, that the traces of the DF to consider remain the same.

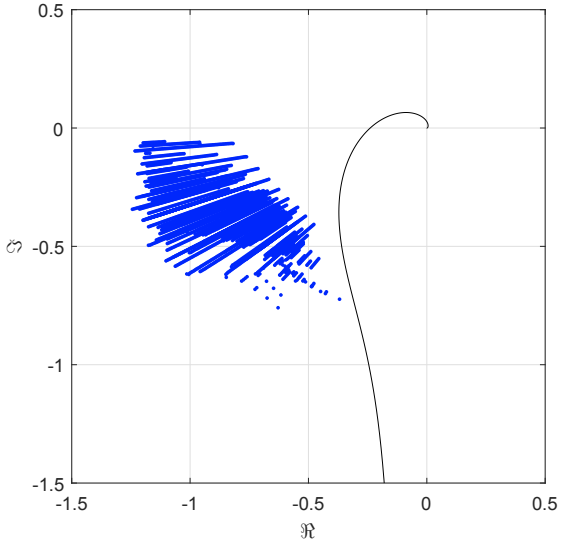

Fig. 7. Traces of $-1/\mathcal{N}$ for $r \in [8, 16]$ and $G_{ol}(s)$ with the detuned controller.

To show this detuning procedure let us introduce the following example.

Example 2. Consider for this example the process and controller from the previous example. As it has been demonstrated, this system presents limit cycle oscillations, and for the sake of this example let us consider that the sampling period is a strong constraint and it cannot be lowered.

As it has been commented before, to avoid limit cycle oscillations, the proposed solution consists in detuning the controller by reducing the proportional gain which assures that the DF traces obtained in the precedent example remain the same.

Thus, we have chosen to reduce the proportional gain K_p in such way that it assures the no intersection with the traces of the inverse negative of the describing function, being the new value $K_p = 0.844$. In Figure 7 it can be seen the Nyquist diagram representing the system with the detuned controller and the DF traces. It can be appreciated that there is no intersection between G_{ol} and the DF traces and thus no limit cycle oscillations are expected to appear.

This has been confirmed through simulation, in Figure 8 it can be observed the response of the controlled output $y(t)$ and the control action $u(t)$ to a unitary step change in the reference input and in the disturbance input $p(t)$ at $t = 50s$, and it can be seen that no limit cycle oscillations appears.

Nevertheless, in some applications the user has some freedom regarding to the choice of the sampling period. In those cases, the controller tunned for the continuous case can be kept and the sampling period can be adjusted to avoid limit cycle oscillations.

Example 3. Consider the same process and controller than in Example 1. To avoid limit cycle oscillations, and if the hardware requirements allows it, we can increase the sampling frequency, fixing for example $T_s = 0.25$ seconds.

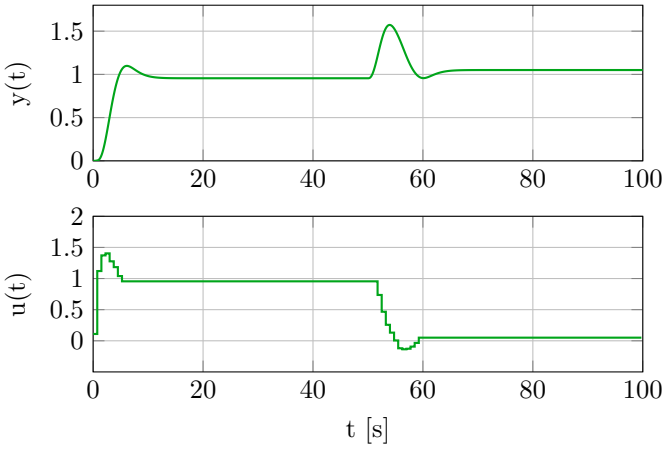

Fig. 8. Experiment considering a unitary step change in the reference input and in the disturbance input at $t = 50$ s. Controlled output in the upper figure and control action in the lower figure.

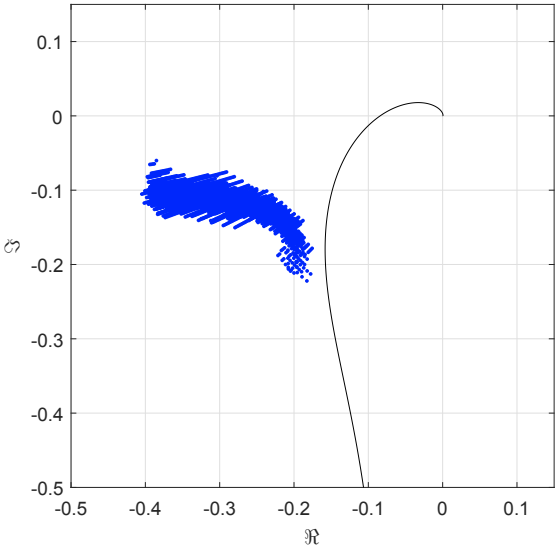

Fig. 9. Traces of $-1/\mathcal{N}$ for $r \in [21, 47]$ and $G_{ol}(s)$ with $T_s = 0.25$.

Making this change, the phase crossover frequency changes, because it modifies the open loop transfer function $G_{ol}(s)$, modifying the range of r to evaluate which now starts at $r_{min} = 21$. As we have seen in the previous section, the effect of increasing r makes the DF traces to be closer and reduce its dispersion. This can be seen in Figure 9, where the traces of $-1/\mathcal{N}$ have been represented for $r \in [21, 47]$, and as it can be seen there is no intersection between those traces and $G_{ol}(s)$, therefore, for this system choosing $T_s = 0.25$ avoids the limit cycle oscillations produced by the discrete controller implementation.

This system has been tested in simulation and as it can be seen in Figure 10 it does not present limit cycle oscillation. In the experiment presented in this figure a unitary step change has been applied to the reference input $y_r(t)$ and to the disturbance input $p(t)$ at $t = 50$ s, and as the DF predicted, no limit cycle oscillation took place.

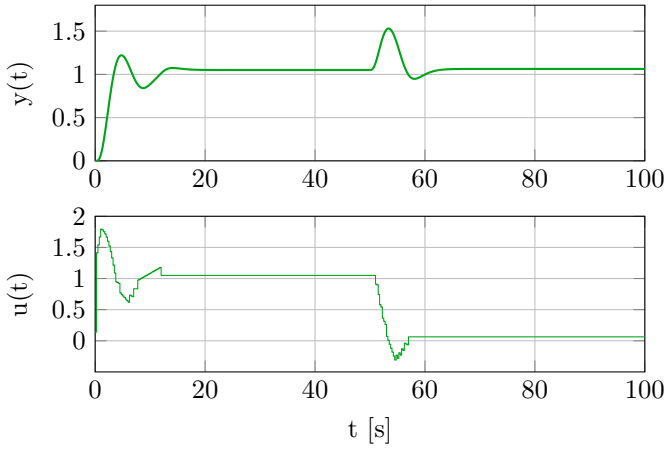

Fig. 10. Experiment considering a unitary step change in the reference input and in the disturbance input at $t = 50$ s. Controlled output in the upper figure and control action in the lower figure.

6. CONCLUSION

In this contribution an initial approach to study the robustness of discrete event based systems is proposed. Unlike other proposals, in this study the controller is supposed to be implemented in a standard control device, and thus, the controller is no longer considered to be continuous for the robustness study.

The proposal is based on the Sampled Describing Function technique, which allows to use some tools of the classical control theory, such as the Nyquist plot, which is used to determine the existence of limit cycle oscillations.

The validity of the approach in predicting steady-state oscillations is shown through several examples in which a system with a controller tuned with a specific tuning method for controllers with a SSOD sampler is used. The predictions made with the Sampled DF are confirmed through simulation.

Finally, some guidelines are given to avoid limit cycle oscillations. Namely, detune the controller by reducing the proportional gain or, in those cases where it is possible increase the sampling period.

REFERENCES

Beschi, M., Dormido, S., Sanchez, J., and Visioli, A. (2012). Characterization of symmetric send-on-delta PI controllers. *Journal of Process Control*, 22(10), 1930–1945.

Beschi, M., Dormido, S., Sanchez, J., and Visioli, A. (2014). Tuning of symmetric send-on-delta proportional-integral controllers. *IET Control Theory Applications*, 8(4), 248–259. doi:10.1049/iet-cta.2013.0048.

Dormido, S., Sánchez, J., and Kofman, E. (2008). Muestreo, control y comunicación basados en eventos. *Revista Iberoamericana de Automática e Informática Industrial RIAI*, 5(1), 5–26.

Gelb, A. and Van der Velde, W.E. (1968). *Multiple-input describing functions and non-linear system design*. McGraw-Hill.

Hägglund, T. and Åström, K.J. (2002). Revisiting the ziegler-nichols tuning rules for PI control. *Asian Journal of Control*, 4(4), 364–380.

Miguel-Escrig, O., Romero-Pérez, J.A., and Sanchis-Llopis, R. (2019). Tuning pid controllers with symmetric send-on-delta sampling strategy. *Journal of the Franklin Institute*.

Ploennigs, J., Vasyutynskyy, V., and Kabitzsch, K. (2010). Comparative study of energy-efficient sampling approaches for wireless control networks. *IEEE Transactions on Industrial Informatics*, 6(3), 416–424.

Romero, J.A. and Sanchis, R. (2016). A new method for tuning PI controllers with symmetric send-on-delta sampling strategy. *ISA transactions*, 64, 161–173.

Romero, J.A., Sanchis, R., and Penarrocha, I. (2014). A simple rule for tuning event-based PID controllers with symmetric send-on-delta sampling strategy. In *Proceedings of the 2014 IEEE Emerging Technology and Factory Automation (ETFA)*, 1–8. doi: 10.1109/ETFA.2014.7005070.

Skogestad, S. (2003). Simple analytic rules for model reduction and PID controller tuning. *Journal of process control*, 13(4), 291–309.

Appendix A. CALCULATION OF $\mathcal{N}$

The sampled describing function which relates the input and output of the non-linear element in the system can be computed in the following way:

$$\mathcal{N} = \frac{\text{Phasor of fundamental component of } \bar{e}^*}{\text{Phasor representation of } e}.$$

Firstly, the phasor representation of e can be easily obtained:

$$e(t) = A\sin(\omega_o t) = A\cos\left(\omega_o t + \frac{3\pi}{2}\right) = \Re\left\{Ae^{j\left(\omega_o t + \frac{3\pi}{2}\right)}\right\}. \tag{A.1}$$

For the phasor representation of the fundamental component of $\bar{e}^*$, an harmonic analysis using Fourier series has been done. Expressing $\bar{e}^*(t)$ as:

$$\bar{e}^*(t) = \bar{e}(t)\cdot\delta_{PT}(t),$$

where the pulse train δ_{PT} is defined as:

$$\delta_{PT}(t) = \sum_{k=-\infty}^{\infty}\delta_D(t-\tau-kT_s),$$

where δ_D is the Dirac delta function, T_s is the sampling period and τ the time lag between the initial zero-crossing of $e(t)$ and the first sample (which is bounded between 0 and T_s).

To obtain the fundamental component of $\bar{e}^*(t)$, firstly we obtain the Fourier series representing $\bar{e}(t)$:

$$\hat{\bar{e}}(t) = -\frac{\delta}{j\pi}\sum_{n=-\infty}^{\infty}\frac{1}{n}\left\{\sum_{i=1}^{m} i\left[e^{-jn\omega_o t_{i+1}} - e^{-jn\omega_o t_i}\right] + \sum_{i=m+1}^{2m-1}(2m-i)\left[e^{-jn\omega_o t_{i+1}} - e^{-jn\omega_o t_i}\right]\right\}e^{jn\omega_o t},$$

where t_n are the times where level switches are produced. And secondly, we obtain the Fourier series representation of δ_{PT} is:

$$\hat{\delta}_{PT}(t) = \frac{1}{T_s}\sum_{k=-\infty}^{\infty}e^{jk\omega_s(t-\tau)}.$$

Multiplying both:

$$\hat{\bar{e}}^*(t) = \frac{-\delta}{j\pi T_s}\sum_{k=-\infty}^{\infty}\sum_{n=-\infty}^{\infty}\frac{1}{n}\left\{\sum_{i=1}^{m} i\left[e^{-jn\omega_o t_{i+1}} - e^{-jn\omega_o t_i}\right] + \sum_{i=m+1}^{2m-1}(2m-i)\left[e^{-jn\omega_o t_{i+1}} - e^{-jn\omega_o t_i}\right]\right\}e^{jn\omega_o t}e^{jk\omega_s(t-\tau)}.$$

To obtain the fundamental harmonic from this expression we have to pay attention to the exponents that imply the variable t, which can be grouped in a single expression:

$$j(n\omega_o + k\omega_s)t - jk\omega_s\tau.$$

Then, the coefficient of t has to be the fundamental frequency, i.e. either $+\omega_o$ or $-\omega_o$. Taking r as the ratio between the oscillation and sampling period ($r = T_o/T_s$), we can obtain the relation between the harmonics of the sampling (k) and of the signal $\bar{e}(t)$ (n) to obtain the fundamental frequency of $\bar{e}^*(t)$:

$$\begin{aligned} n\omega_o + k\omega_s = \omega_o \qquad & n\omega_o + k\omega_s = -\omega_o \\ n + k\frac{\omega_s}{\omega_o} = 1 \qquad & n + k\frac{\omega_s}{\omega_o} = -1 \\ n = 1 - kr \qquad & n = -1 - kr \end{aligned}$$

Thus the relation of harmonics to consider are both $n = 1-kr$ and $n = -1-kr$. The expression of the fundamental harmonic of $\bar{e}^*(t)$ is:

$$\hat{\underline{\bar{e}}}^*(t) = \frac{j\delta}{\pi T_s}\sum_{k=-\infty}^{\infty}\left\{\frac{e^{j\omega_o t}}{1-rk}(\mathcal{A}+\mathcal{B}) - \frac{e^{-j\omega_o t}}{1+rk}(\mathcal{C}+\mathcal{D})\right\}e^{-jk\omega_s\tau}, \tag{A.2}$$

where:

$$\mathcal{A} = \sum_{i=1}^{m} i\left[e^{-j(1-rk)\omega_o t_{i+1}} - e^{-j(1-rk)\omega_o t_i}\right],$$

$$\mathcal{B} = \sum_{i=m+1}^{2m-1}(2m-i)\left[e^{-j(1-rk)\omega_o t_{i+1}} - e^{-j(1-rk)\omega_o t_i}\right],$$

$$\mathcal{C} = \sum_{i=1}^{m} i\left[e^{-j(-1-rk)\omega_o t_{i+1}} - e^{-j(-1-rk)\omega_o t_i}\right],$$

$$\mathcal{D} = \sum_{i=m+1}^{2m-1}(2m-i)\left[e^{-j(-1-rk)\omega_o t_{i+1}} - e^{-j(-1-rk)\omega_o t_i}\right].$$

The values of $\mathcal{N}$ can be calculated using the equations (A.1) and (A.2).